Journal of Metals, Materials and Minerals, 37(1), e2823, 2027

Commercial nail polish-based single-electrode triboelectric nanogenerator for mechanical energy harvesting and water droplet energy conversion

Subrat BHOL[1], Basanta Kumar PANIGRAHI[1,*], Nakul Charan SAHU[1], Arjun KUMAR[2], Archana PANDA[3], and P. L. DEEPTI[4]

[1] *Department of Electrical Engineering, Siksha O Anusandhan (deemed to be University), Bhubaneswar 751030, India*
[2] *Department of Electrical Engineering, Sri Phanishwar Nath Renu Engineering College Araria, DSTTE Bihar 854318, India*
[3] *Department of Electronics and Communication Engineering, ITER Siksha O Anusandhan (deemed to be University), Bhubaneswar 751030, India*
[4] *Veer Surendra Sai University of Technology, Burla, 768018, India*

***Corresponding author e-mail**: basanta1983@gmail.com

Received date:
27 July 2026
Revised date:
25 August 2026
Accepted date:
26 September 2026

Keywords:
Triboelectric nanogenerator;
Nail polish;
Mechanical energy harvesting;
Electronics;
Water droplet energy harvesting

Abstract

Triboelectric nanogenerators (TENGs) have brought new opportunities to realize relevant low-frequency mechanical energy self-powered systems, it is still a challenge and holds back the development of simple, low-cost, and scalable triboelectric materials. In this work, a triboelectric layer is made of commercially available nail polish used to fabricate a single-electrode TENG (abbreviated as N-TENG). The device was driven in single-electrode mode and exhibited an open-circuit voltage of 195 V, short-circuit current of 1300 nA, and maximum output power of 51.09 μW at an external load resistance of 500 MΩ. The electrical performance illustrates how nail polish acts as a feasible triboelectric material used for energy conversion, especially due to its availability. The practical applicability was validated through powering a commercial calculator, and other experiments proved that the device could harvest energy from free-falling water droplets under gravitational potential, indicating further applications for rain-energy harvesting. With the advantages of simple fabrication process, low-cost materials and acceptable electrical performance, the proposed N-TENG is practical for self-powered electronics and environmental energy harvesting.

1. Introduction

Low-frequency mechanical energy can be effectively converted into electrical energy using triboelectric nanogenerators (TENGs). Due to their simple device architecture, light weight, low fabrication cost, and the capability of using various types of materials, TENGs have received considerable attention for sustainable energy harvesting and self-powered sensing applications [1–4]. In recent years, considerable effort has been devoted to improving the output performance of TENGs by exploring new triboelectric materials and device configurations [5–7]. The choice of triboelectric materials is crucial to the charge-generation capability and overall efficiency of a TENG. Therefore, many natural, synthetic, biodegradable, and waste materials have been investigated as triboelectric layers [8–12]. In addition to improving device performance, the use of unconventional materials can offer other benefits, such as low-cost fabrication, material availability, environmentally friendly properties, and ease of processing [13–17]. Therefore, the continuous exploration of new triboelectric materials is crucial for expanding the practical applications of TENG technology. Recently, some unconventional materials have been investigated for TENG applications. For example, Panda *et al.* developed a flexible and eco-friendly rice paper-based RP/PDMS TENG for efficient biomechanical energy harvesting, with a maximum output of 305 V, 2.6 μA, and 29 nC [18]. Similarly, the discarded facial mask-based triboelectric nanogenerator (FM-TENG) was fabricated by Xia *et al.*, exhibiting a high output of 1037 V, 37.48 μA, and a power density of 727.78 $\mu W \cdot cm^{-2}$, demonstrating its potential in biomechanical energy harvesting and self-powered touch sensing. The skin-friendly device can power commercial electronics and 150 LEDs, showing its potential for wearable electronics and smart wireless sensor networks. Triboelectric materials based on paint have also been investigated for energy harvesting applications [19]. Yun *et al.* fabricated a paint-based triboelectric nanogenerator (PBT) using a spray-deposition method with improved electrical output and successful applications in intrusion detection and secure keypad systems [20].

Nail polish is an interesting but relatively underexplored class of coating materials for triboelectric energy harvesting. Commercial nail paints consist of polymeric binders, pigments, plasticizers, and various functional additives that can affect the surface charge generation during triboelectric interactions [20–22]. Moreover, nail paints are widely available and inexpensive and can be easily applied to various substrates using a simple brush-coating process without the need for sophisticated fabrication equipment. These features make nail paint a promising candidate for the development of facile and scalable triboelectric devices [23–25]. Although the triboelectric behavior of nail-paint-based materials has been demonstrated previously, most

of the reported work has focused on conventional vertical contact-separation device architectures. The single-electrode configuration, which has been less studied, offers the advantages of simpler device design, operational flexibility, and applicability to energy harvesting from freely moving objects [26–29]. Additionally, the triboelectric properties of nail-paint-coated surfaces in contact with liquid media have not been systematically studied [30,31]. Such solid–liquid triboelectric interactions are of particular importance, as many abundant energy sources, such as rain droplets, flowing water, and liquid impacts, can be harnessed for sustainable energy harvesting [32,33].

We report here on the design and systematic evaluation of a single-electrode nail-paint triboelectric nanogenerator (N-TENG) with a nail-paint-coated active layer. The fabricated N-TENG produces the output voltage and current of 195 V and 1300 nA, respectively. The device's electrical output characteristics under biomechanical excitation are studied, and the effects of operating frequency and environmental conditions on performance are investigated. Importantly, the applicability of the nail-paint coating is further extended from solid-solid contact to solid-liquid triboelectric interaction using water droplets. Thus, the objective of this work is not to introduce nail paint as a new triboelectric material, but to extend its application to a single-electrode architecture and demonstrate its operation under both solid–solid and solid–liquid mechanical interaction. The results offer an experimentally accessible approach for the use of commercially available nail paint in simplified and versatile triboelectric energy harvesting systems.

2. Material and methods

2.1 Materials

The nail polish used in this study was commercially available Zudio nail polish purchased from Amazon and used without any further modification, and polyethylene terephthalate (PET) sheet, aluminum tape, and copper wire were cut to the required size and used to fabricate the TENG.

2.2 TENG fabrication method

The TENG device fabrication was started by preparing a supporting substrate of PET sheet of 4 cm × 4 cm. The tribopositive active layer was prepared by brush-coating a thin layer of nail paint on an aluminum tape electrode of 3 cm × 3 cm. The coated electrode was then left to dry at room temperature to ensure a uniform triboelectric surface. A copper wire was then attached to the aluminum tape to make an electrical connection. The assembled electrode was then attached on the PET substrate to obtain a mechanically stable device structure suitable for electrical characterization and energy harvesting applications.

2.3 Characterization techniques

The electrical characterization of the fabricated TENG was carried out using Keithley 6514 electrometer interfaced with LabVIEW based data acquisition system. A LINMOT linear motor (USA) was used to repeatedly mechanically stimulate the samples under uniform testing conditions. The surface characteristics and microstructural features of the samples were investigated by field-emission scanning electron microscopy (FESEM, ZEISS).

3. Results and discussion

The common components in any nail paint include the film-forming polymer (resin), plasticizers, and solvents. The film-forming polymer forms a smooth, hard layer of the paint film on the nail, while the resin ensures the paint adheres to the nail surface. Nitrocellulose is the most important film-forming polymer, present in all nail paints. The plasticizers make the layer flexible so that it does not break easily. Common plasticizers include camphor, dibutyl phthalate, phenyl phosphates, and benzoates. The solvent is used as a medium to create uniformity in smell and to make the mixture homogeneous. Examples of solvents include alkyl acetates and acetone. The chemical structure of these compounds can be depicted in Figure 1(a–b) illustrates the device fabrication process of the single-electrode-based N-TENG. Here, the nail paint serves as the tribopositive active layer, and nitrile gloves serve as the tribonegative layers, due to their tendency to accept electrons. The operational mechanism of the N-TENG is depicted in Figure 1(c). The nail paint and nitrile gloves have opposite triboelectric polarities; consequently, when they contact each other, charge transfers between the two materials, creating equal and opposite charges. As the two materials separate, an electrical potential difference builds up at the electrode, causing electrons to flow from the external circuit. Eventually, the two layers become totally separated, and electron flow stops as the system reaches an equilibrium state. When the two layers again start to make contact, the electrons move in the opposite direction, and this cycle of contact and separation produces an alternating current.

Figure 2(a) shows the FESEM image of the nailpaint thin film, it reveals a relatively smooth and uniform morphology of the surface. Furthermore, the absence of major cracks or delamination indicates the good film integrity, which is advantageous for maintaining consistent triboelectric performance during repeated contact-separation cycles. The thickness of the dried nail-paint layer was measured from the cross-sectional SEM image and was approximately 82.5 μm, as shown in Figure S1. The elemental mapping analysis was performed to analyze the distribution of the constituent elements in the coated film. As can be seen in Figure 2(b–c), carbon, oxygen, and nitrogen are uniformly distributed across the surface, with no obvious elemental segregation. Such a homogeneous distribution indicates the formation of a continuous coating layer and demonstrates the compositional consistency of the triboelectric material. FTIR spectroscopy was used to study chemical functionalities present in the commercial nail-paint coating. Figure S2 shows the FTIR spectrum of the dried nailpaint film. The broad absorption band around 3479 cm^{-1} could be assigned to O–H stretching vibration and the bands between 2950 cm^{-1} and 2850 cm^{-1} to C–H stretching vibrations. The band around 1638 cm^{-1} can be assigned to the asymmetric stretching vibration of the NO_2 group, and the band around 1280 cm^{-1} to the symmetric stretching vibration of NO_2. Additional bands from 1200 cm^{-1} to 1000 cm^{-1} are attributed to C–O/C–O–C stretching vibrations. FTIR spectroscopy showed that the presence of hydroxyl–, C–H–, and C–O/C–O–C containing functionalities in the nail-paint film can influence the surface electronic properties and the interfacial charge-transfer behavior, which may contribute to the relatively tribopositive nature of the nail-paint surface. Figure 2(d) presents the variation of the dielectric constant with frequency for the nailpaint layer.

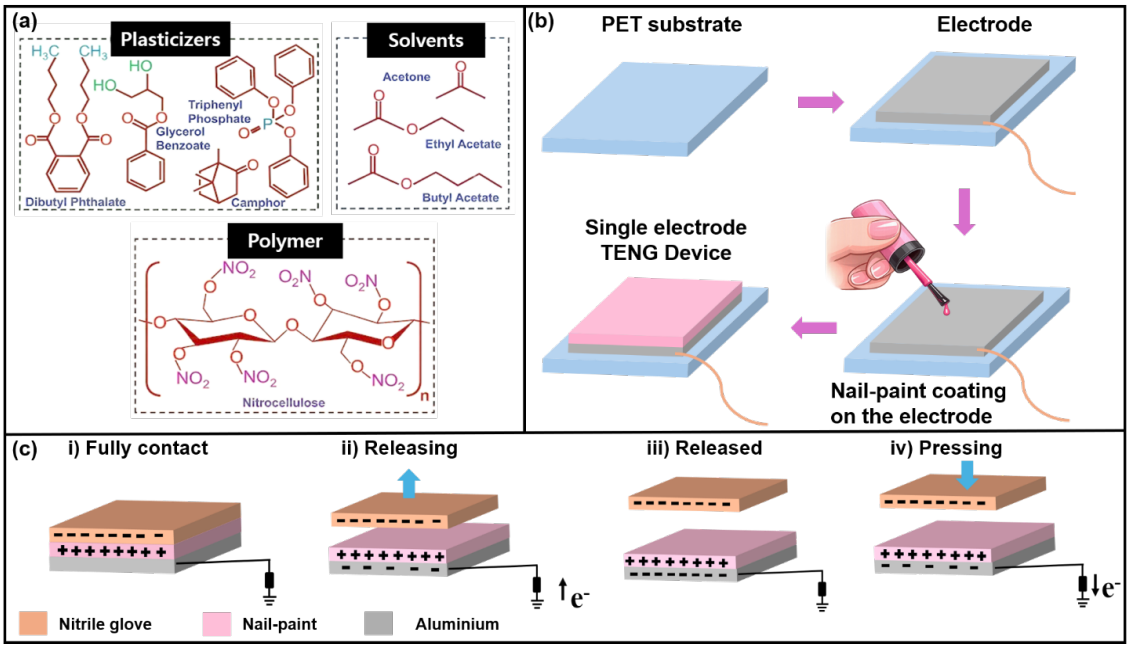


Figure 1. (a) Chemical structures of some common ingredients of nail paints, (b) stepwise device fabrication process of N-TENG, and (c) operational mechanism of the N-TENG.

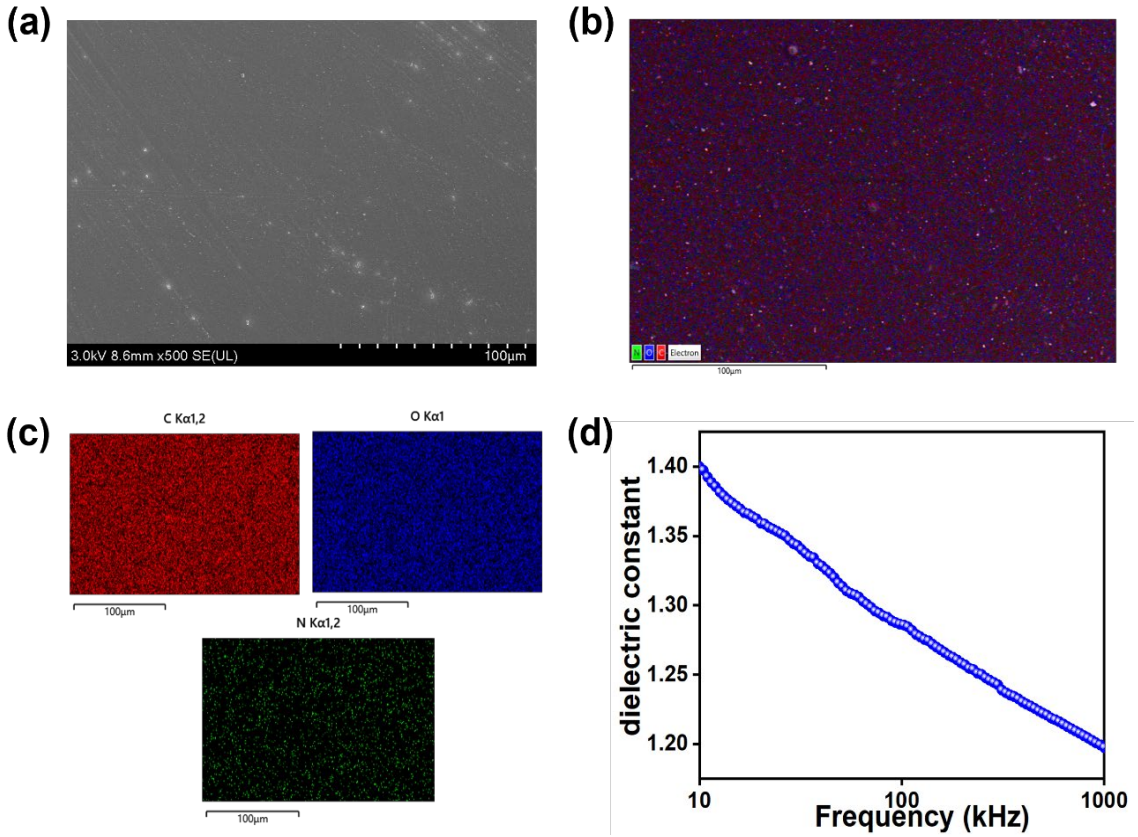


Figure 2. (a) Surface morphology, (b–c) elemental distribution maps, and (d) dielectric constant of the nailpaint layer.

The electrical performance of the N-TENG has been examined to evaluate the energy harvesting capabilities of nailpaint. The key electrical parameters, including voltage, current, and charge, are measured under continuous mechanical stimulation under controlled operational conditions for reliable, accurate data. The mechanical stimulation is given by the linear motor with a frequency of 1 Hz and a force of 5 N. Under these operational conditions, the device produced a maximum open-circuit voltage of 195 V, a short-circuit current of 1300 nA, and a transferred charge of 20 nC as shown in Figure 3(a–c). The high electrical output indicates the effective operation of contact

electrification and electrostatic induction processes, suggesting the device's potential for energy-harvesting applications. Furthermore, the device was tested for long-term stability, the device showing no degradation in performance over the 1000 continuous cycles as depicted in Figure 3(d). In addition, the device exhibited stable output over a 15 day period, with consistent voltage responses recorded on 1 day, 2 day, 5 day, 7 day, 10 day, and 15 under identical experimental conditions, as shown in Figure S3. This excellent performance shows the device's robustness and operational capabilities for long-term applications. In addition, we conducted a comprehensive evaluation of the fabricated TENG under different excitation frequencies while maintaining a constant applied force. As the operating frequency increased from 0.4 to 1.8 Hz, both the voltage and current output showed an increasing trend, as shown in Figure 3(e–f). The increase in electrical output is due to the increases rate of contact separation between the triboelectric layers, which leads to more charge transfer events within a given time frame. These results suggest that the operating frequency is a critical parameter in determining the energy harvesting capacity of the TENG device. The output voltage of the device with the different opposite layers under identical conditions is presented in Figure S4.

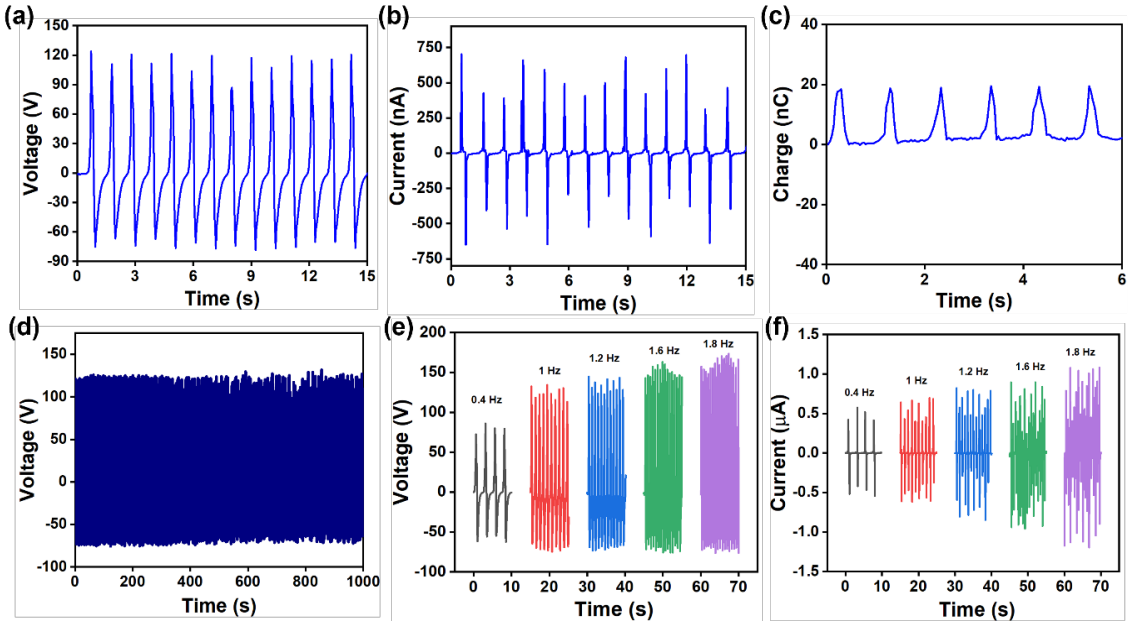


Figure 3. The output performance of the N-TENG (a) voltage, (b) current, (c) charge, (d) operational long-term stability of the device, the frequency-dependent response of the N-TENG (e) voltage, and (f) current, respectively.

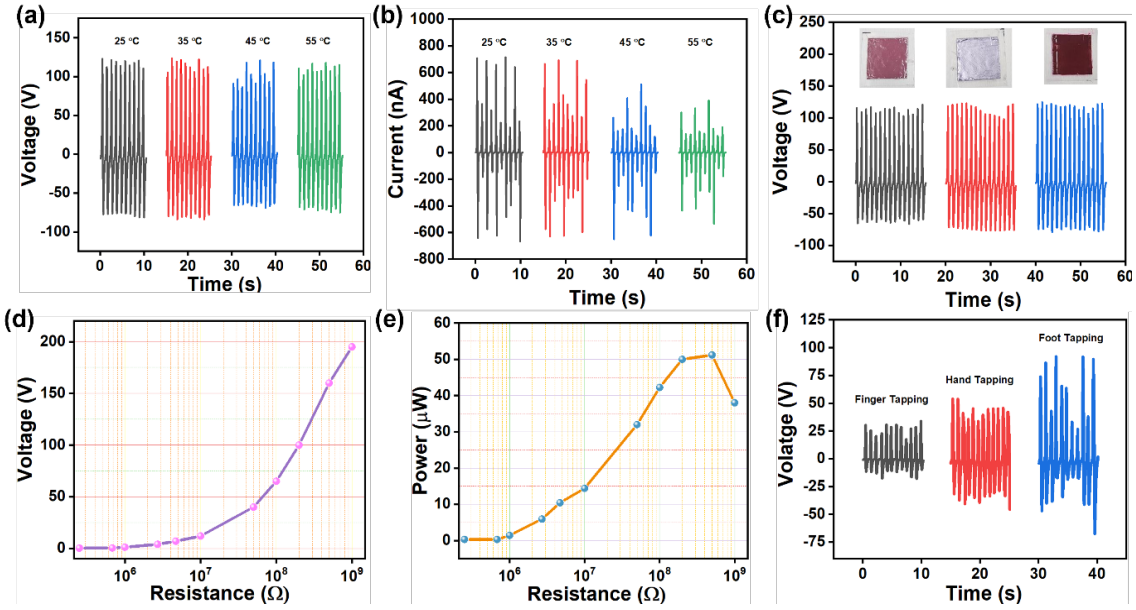


Figure 4. Effect of temperature on the N-TENG (a) output voltage, (b) current measured under varying temperatures, (c) output voltage of the different commercial brands nailpaint coating layers, (d,e) device output voltage and power at different external loads, and (f) biomechanical energy harvesting performance of the N-TENG.

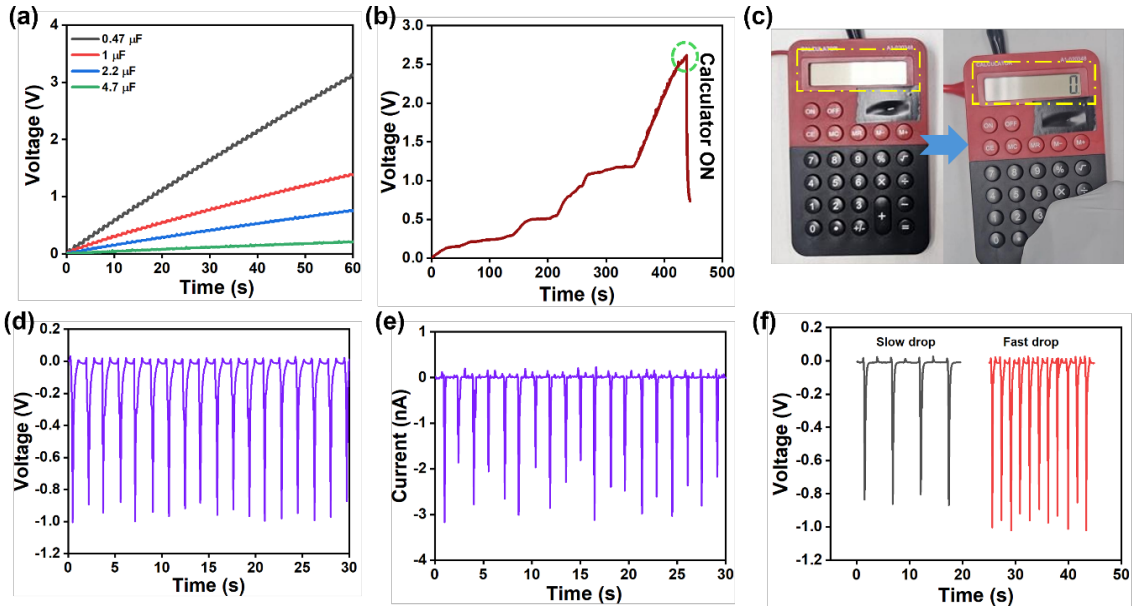


Figure 5. (a) Charging performance of capacitors with different capacitances using the N-TENG, (b) charging of a 4.7 μF capacitor by hand tapping for powering a calculator, (c) digital photographs of the calculator in the OFF and ON states, (d) output voltage, (e) output current of the solid-liquid N-TENG, and (f) comparison of the device output under slow and fast droplet impact conditions.

To evaluate the thermal stability of the TENG device, the temperature-dependent characteristics were investigated. The output voltage and current of the TENG device at different temperature was showcased in Figure 4(a–b). The voltage and current output show stable output up to 35°C, but as the temperature increases, the device's output shows a slight downward trend. The decrease may be due to the increased mobility of charge carriers and increased dielectric losses in the nail-paint layer at higher temperatures [34]. Hence, some of the triboelectric charges dissipate faster instead of accumulating on the surface, resulting in a reduction in the effective surface charge density and, therefore, a reduction in the measured electrical output. To examine the device reproducibility and the reliability of the results, by using the 3 different brands of nailpaint, we fabricated the devices, and the performance is depicted in Figure 4(c). The impact of the external load on the N-TENG has been evaluated by changing the resistance from 250 KΩ to 1 GΩ, and the generated output voltage was measured, as shown in Figure 4(d). With an increase in the resistance value, the output voltage increases, following Ohm's law. Figure 4(e) presents the output power of the N-TENG as a function of external load resistance. The device achieves a peak power of 51.09 μW at an external load resistance of 500 MΩ. To check the device energy harvesting capacity of the device from biomechanical motion, we conducted an experiment in which we used mechanical motion from human daily life activities, such as finger, hand, and foot tapping. The resultant output performance of the device is plotted in Figure 4(f).

The capacitor-charging performance of the N-TENG with different capacitances is shown in Figure 5(a). The smaller-capacitance capacitor charges faster than the larger-capacitance one but stores less energy. To assess the practical applicability of the N-TENG, the 4.7 μF capacitor was charged by hand tapping as shown in Figure 5(b). The digital image of the calculator in the ON and OFF states is shown in Figure 5(c). This experiment demonstrates the capability of the device to power small electronic devices. Table S1 summarizes a comparison of the proposed nail-paint-based TENG with recently reported paint- and coating-based TENGs.

In addition to solid-solid triboelectrification, the N-TENG was examined under solid-liquid contact to assess its potential for water droplet-based energy harvesting. The electrical response of the N-TENG was evaluated using the periodic excitation of the water droplet. When the water droplet meets a nail paint-coated surface, charge redistribution occurs at the solid-liquid interface, generating an electrical potential difference between the electrodes. The continuous arrival and departure of droplets generate repeatable voltage and current signals. Figure 5 (d–e) presents the voltage and current generated by the N-TENG under droplet excitation. The device produces an output voltage of 1 V and a current of 3 nA. To investigate the effect of droplet frequency on the device's electrical performance, measurements were carried out at different droplet frequencies, as shown in Figure 5(f). The output voltage of the N-TENG was measured at different falling heights of the droplets (1 cm, 2 cm, and 3 cm), as shown in Figure S5. However, with the increase in droplet falling height, the impact velocity of the droplet increases, which leads to better liquid-solid contact and a higher output voltage. The observed performance demonstrates the versatility of the fabricated N-TENG in harvesting solid-solid and solid-liquid mechanical energy.

4. Conclusions

The present work demonstrates the use of readily available nail polish as the triboelectric active material to create an N-TENG. The fabrication method is extremely easy and fast and involves coating the desired substrate with a single layer of nail paint, just as in cosmetics. In the pairing of nail-paint TENG with an aluminum electrode, the voltage was approximately 195 V, the current 1300 nA, and the output power nearly 51.09 μW at an external load of 500 MΩ in single-electrode operation mode. Furthermore, the N-TENG was used to

power a calculator, and energy harvesting was achieved by placing water droplets. These open the avenue for TENG as a sustainable power source and for energy harvesting from natural sources, such as rainfall. These unique characteristics introduce a convenient "paint-and-generate" approach to energy harvesting, enabling the rapid fabrication of portable and customizable TENG devices on virtually any surface using a simple brush-coating process.

References

[1] T. Cheng, J. Shao, and Z. L. Wang, "Triboelectric nanogenerators," *Nature Reviews Methods Primers,* vol. 3, no. 1, p. 39, 2023.

[2] C. Wu, A. C. Wang, W. Ding, H. Guo, and Z. L. Wang, "Triboelectric nanogenerator: A foundation of the energy for the new era," *Advanced Energy Materials,* vol. 9, no. 1, p. 1802906, 2019.

[3] S. Hajra, S. Pal, K. R. Kaja, Y. Choi, S. Panda, B. K. Panigrahi, H. J. Kim, and A. F. Wistrand, "Biodegradable single-electrode triboelectric nanogenerator for self-powered robotic texture sensing," *Materials Chemistry Frontiers,* 2026.

[4] U. K. Khanapurarm, G. M. Rani, S.Panda, T. Charoonsuk, K. Mistewicz, S. Hajra, K. R. Kaja, R. Umapathi, S. Sriphan, J. Jała, H. Divi, A. Smalcerz, M. Belal, P. Jaahnavi, M. Safarkhani, H. Kim, Y. K. Mishra, H. J. Kim, Y. S. Huh, N. Vittayakorn, B. Nowacki, S. K. Ravi, S. J. Eichhorn, M. F. Craciun, A. Borras, H. Khanbareh, J. Qin, Ra. K. Rajaboina,"Harvesting energy from friction: The revolutionary decade of triboelectric nanogenerators," *Advanced Powder Materials,* vol. 5, no. 2, p. 100373, 2026.

[5] K. R. Kaja, S. Hajra, U. Pharino, P. S. Bhosale, S. Panda, M. A. Belal, S. Sriphan, U. K. Khanapuram, N. Vittayakorn, H. J. Kim, "High-performance droplet driven electrification for self-powered real-time nitrate monitoring in agricultural water systems," *Journal of Science: Advanced Materials and Devices,* p. 101154, 2026.

[6] S. Hajra, A. M. Padhan, B. K. Panigrahi, P. Pakawanit, Z. Jagličić, N. Vittayakorn, Y. K. Mishra, S. Lee, and H. J. Kim, "Unleashing the potential of morphotropic phase boundary based hybrid triboelectric–piezoelectric nanogenerator," *Journal of Materiomics,* vol. 10, no. 4, pp. 792–802, 2024.

[7] R. Muddamalla, U. K. Khanapuram, R. K. Rajaboina, and H. Divi, "A comprehensive review of zinc vanadate materials: from synthesis to multifunctional devices," *Coordination Chemistry Reviews,* vol. 568, p. 218437, 2026.

[8] M. Niharika, R. Garlapallya, K. Ruthvik, M. Velaga, and B. M. Rao, "Hydrogen production on g-C_3N_4 nanoflakes via photoelectrochemical water splitting," *Materials Today: Proceedings,* 2023.

[9] N. Anitha, K. Jayanthi, R. Muddamalla, A. A. Sharma, N. Jayarambabu, A. Akshaykranth. K. Babu, T. Venkatappa Rao, D. Dinakar, and H. Divi, "Origin of the active luminescence from Sm 3^+-activated borate phosphors: A correlational study of trap states and decay kinetics," *New Journal of Chemistry,* vol. 47, no. 3, pp. 1472–1478, 2023.

[10] S. A. Behera, S. Hajra, S. Panda, A. K. Sahu, P. Alagarsamy, Y. K. Mishra, H. J. Kim, P. G. R. Achary, "Synergistic energy harvesting and humidity sensing with single electrode triboelectric nanogenerator," *Ceramics International,* vol. 50, no. 19, Part B, pp. 37193–37200, 2024.

[11] K. U. Kumar, S. Hajra, G. M. Rani, S. Panda, R. Umapathi, S. Venkateswarlu, H. J. Kim, Yogendra Kumar Mishra, and R. R. Kumar, "Revolutionizing waste-to-energy: Harnessing the power of triboelectric nanogenerators," *Advanced Composites and Hybrid Materials,* vol. 7, no. 3, p. 91, 2024.

[12] M. Velpula, A. Kaki, K. U. Kumar, and R. K. Rajaboina, "Upcycling waste fruit protective net foam into polyethylene films for sustainable triboelectric energy harvesting," *Advanced Sustainable Systems,* vol. 10, no. 8, p. e70615, 2026.

[13] R. Zhang, and H. Olin, "Material choices for triboelectric nanogenerators: A critical review," *EcoMat,* vol. 2, no. 4, p. e12062, 2020.

[14] Y. Li, Y. Luo, H. Deng, S. Shi, S. Tian, H. Wu, J. Tang, C. Zhang, X. Zhang, J.-W. Zha, and S. Xiao,"Advanced dielectric materials for triboelectric nanogenerators: principles, methods, and applications," *Advanced Materials,* vol. 36, no. 52, p. 2314380, 2024.

[15] S. Hajra, K. R. Kaja, S. Panda, M. A. Belal, B. K. Panigrahi, P. Pakawanit, and H. J. Kim,"Waste based triboelectric nanogenerator for energy harvesting and self-powered sensors," *Journal of Cleaner Production,* vol. 509, p. 145591, 2025.

[16] V. L. Suneetha, V. Mahesh, K. Uday Kumar, and R. R. Kumar, "Upcycling medical tablet blister waste into high-performance triboelectric nanogenerators for sustainable energy harvesting," *Nanoenergy Advances,* vol. 5, no. 4, p. 19, 2025.

[17] A. Kaki, V. Mahesh, M. Navaneeth, U. K. Khanapuram, R. R. Kisannagar, I. Jung, And R. R. Kumar, "Upcycling expired silicone sealants into high-performance triboelectric nanogenerators for sustainable energy harvesting and smart infrastructure safety systems," *Energy Technology,* vol. 14, no. 2, p. e202502152, 2026.

[18] S. Panda, S. Hajra, P. S. Bhosale, M. A. Belal, K. R. Kaja, H. J. Kim, and K. Lee, "Triboelectric energy harvesting from rice paper/PDMS under extreme humidity environments," *Materials Letters,* p. 139971, 2025.

[19] K. Xia, and Z. Xu, "Applying a triboelectric nanogenerator by using facial mask for flexible touch sensor," *Sensors and Actuators A: Physical,* vol. 331, p. 112710, 2021.

[20] J. Yun, I. Kim, M. Ryoo, Y. Kim, S. Jo, and D. Kim, "Paint based triboelectric nanogenerator using facile spray deposition towards smart traffic system and security application," *Nano Energy,* vol. 88, p. 106236, 2021.

[21] M. Tiwari, and D. Bharti, "Cosmetics-to-energy: Paintable and robust triboelectric nanogenerator based on nail-paints," *Advanced Functional Materials,* p. e75418, 2026.

[22] S. Mishra, M. Rakshita, H. Divi, S. Potu, and R. K. Rajaboina, "Unique contact point modification technique for boosting the performance of a triboelectric nanogenerator and its application in road safety sensing and detection," *ACS Applied Materials & Interfaces,* vol. 15, no. 27, pp. 33095–33108, 2023.

[23] J. Fu, K. Xia, and Z. Xu, "A triboelectric nanogenerator based on human fingernail to harvest and sense body energy," *Microelectronic Engineering,* vol. 232, p. 111408, 2020.

[24] A. Panda, B. K. Panigrahi, S. G. Mohanty, and K. R. Kaja, "Upcycled waste-derived triboelectric nanogenerator for sustainable energy harvesting," *Journal of Metals, Materials and Minerals,* vol. 35, no. 4, p. e2474, 2025.

[25] M. Rakshita, A. A. Sharma, P. P. Pradhan, K. D. Prasad, M. Srinivas, and D. Haranath, "Fabrication and characterization of rare earth-free nanophosphor based devices for solid-state lighting applications," *Materials Advances,* vol. 6, no. 10, pp. 3203-3219, 2025.

[26] A. Panda, K. K. Das, K. R. Kaja, M. Belal, and B. K. Panigrahi, "Single electrode mode triboelectric nanogenerator for recognition of animal sounds," *Journal of Metals, Materials and Minerals,* vol. 34, no. 4, pp. 2170–2170, 2024.

[27] J. A. L. Jayarathna, and K. R. Kaja, "Energy-harvesting device based on lead-free perovskite," *AI, Computer Science and Robotics Technology,* 2024.

[28] S. A. Behera, S. Panda, S. Hajra, B. K. Panigrahi, H. J. Kim, and P. G. R. Achary, "EVA/PZT-composite-based triboelectric nanogenerator for energy harvesting," *Energy Technology,* vol. 11, no. 9, p. 2300469, 2023.

[29] S. A. Behera, H.-G. Kim, I. R. Jang, S. Hajra, S. Panda, N. Vittayakorn, H. J. Kim, P. G. R. Achary, "Triboelectric nanogenerator for self-powered traffic monitoring," *Materials Science and Engineering: B,* vol. 303, p. 117277, 2024.

[30] K. R. Kaja, S. Hajra, S. Panda, M. A. Belal, U. Pharino, H. Khanbareh, N. Vittayakorn, V. Vivekananthan, C. Bowen, and H. J. Kim, "Exploring liquid-solid interface based triboelectrification, structures, and applications," *Nano Energy,* vol. 131, p. 110319, 2024.

[31] K. R. Kaja, S. Hajra, S. Panda, M. Belal, S. Nam, P. Pakawanit, B. K. Panigrahi, H. Khanbareh, C. Bowen, J. Yu, and H. J. Kim, "Waste polyethylene-coated fabrics for dual-mode interfaces triboelectrification for self-powered sensors," *Results in Engineering,* p. 107111, 2025.

[32] P. S. Bhosale, S. Hajra, S. Panda, K. R. Kaja, M. Belal, S. M. Jeong, and H. J. Kim, "Self-powered sucrose detection using a superhydrophobic liquid–solid triboelectric nanogenerator," *Materials Chemistry Frontiers,* vol. 10, no. 9, pp. 1409–1417, 2026.

[33] K. R. Kaja, S. Hajra, S. Panda, M. A. Belal, P. Pakawanit, N. Vittayakorn, C. R Bowen, H. Khanbareh, and H. J. Kim, "Triboelectrification based on the waste waterproof textiles for multisource energy harvesting," *Advanced Sustainable Systems,* vol. 9, no. 5, p. 2400678, 2025.

[34] L. Lu, J. Wu, Y. Zhang, C. Liu, Y. Hu, B. Chen, Y. Zhu, and Y. Mao, "Noncontact 3D gesture recognition enabled VR human–machine interface via electret-nanofiber-based triboelectric sensor," *Nano Research,* vol. 18, no. 11, p. 94907924, 2025.